Gold and Base Metal Mineralization near Kitsumkalum Lake, North of Terrace, West-Central British Columbia

By M.G. Mihalynuk[1] and R.M. Friedman[2]

Keywords: intrusive-related gold mineralization, gold-silver-lead, carbonate alteration, metamorphism, structural deformation, U-Pb geochronology, crustal extension

INTRODUCTION

Geological and geochemical indications of an environment prospective for gold deposits are found in an area extending approximately 12 km east and west of Kitsumkalum Lake in west-central British Columbia (Fig. 1). More than 20 gold mineral occurrences, some with silver, are located within the area, including two with minor past production and an active placer operation. Most occurrences are gold-arsenic-quartz or base and precious-metal quartz veins that are presumably related to one of the many stocks and plutons in the area (Fig. 1). Carbonate alteration envelopes are ubiquitous around sheeted precious-metal–bearing quartz veins (±arsenopyrite-pyrite-sphalerite-galena-chalcopyrite). Regional geochemical stream sediment surveys show elevated gold, mercury and arsenic in the Kitsumkalum area (bismuth and antimony were not analyzed; BC Ministry of Energy and Mines, 2001).

Since 2002, Eagle Plains Resources Ltd. has conducted mineral exploration in the area, primarily west of Kitsumkalum Lake. In 2004, Bootleg Exploration Inc. (a wholly owned subsidiary of Eagle Plains Resources Ltd.) and the British Columbia Ministry of Energy and Mines entered into a partnership agreement aimed at evaluating the regional potential for intrusive-related gold mineralization, both on their Kalum property and around plutons to the east. Geological field investigations were focused on interiors and contacts of intrusive bodies associated with gold mineralization and lode vein occurrences.

In this report, we use the following nomenclature conventions. 'Kitsumkalum area' refers to the areas of the Kitsumkalum valley that lie within an ~12 km radius of Kitsumkalum Lake. 'Kalum area' refers the part of the 'Kitsumkalum area' that lies west of the lake, principally the 'Kalum property', centred west of Mount Allard, as well as the 'LCR property', on the ridges south of the lower stretches of the Little Cedar River. A possible source of confusion arises over the historical use of 'Kalum' and 'Kalum Lake', which are names of developed prospects on the northeast and southwest shores of Kitsumkalum Lake.

ACCESS

The Kalum area is centred approximately 35 km north-northwest of Terrace in west-central British Columbia. With a population of nearly 14 000, Terrace supports a regional airport, rail yard, and most other amenities. It is located at the confluence of the Skeena, Zymoetz and Kitsumkalum Rivers, and at the junction of Highways 6 and 37. Excellent road access is afforded by logging roads that extend off of the new, paved Nisga'a Highway and the old gravel-surfaced Aiyansh Highway on the east and west sides of the Kitsumkalum valley. Steep alpine topography

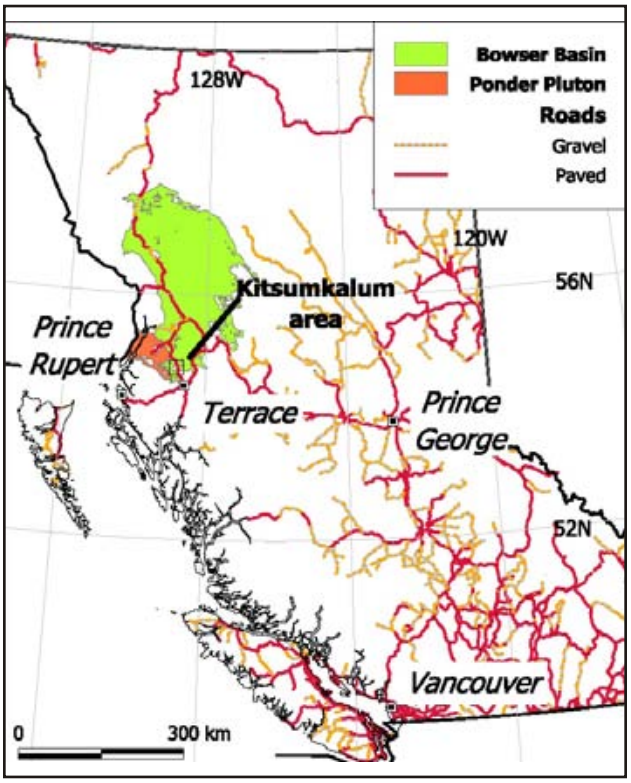

Figure 1. Location of the Kalum project area, 35 km north of Terrace. Geology from Massey (2004).

[1] *British Columbia Ministry of Energy and Mines, e-mail: Mitch.Mihalynuk@gems5.gov.bc.ca*

[2] *Pacific Centre for Isotopic and Geochemical Research, Department of Earth and Ocean Sciences, University of British Columbia*

and dense temperate rainforest, both characteristic of the area, can prove logistically challenging for travelling even short distances from existing access routes.

OBJECTIVES

This report is a summary of field and laboratory data acquired from the Kalum fieldwork completed in 2004. We include the results and interpretations of geological mapping, petrographic and geochemical analysis and geochronological investigations. Objectives are to

describe and sample the mineralized occurrences;

determine what intrusive phases, if any, are associated with gold mineralization, and attempt to establish field criteria that link the intrusive phase(s) to mineralization;

establish a geochronological framework for mineralization and/or mineralizing intrusive phases; and

investigate petrographic evidence that constrains the mineralizing event(s).

METHODS

Fieldwork was conducted over an 18-day period in mid to late August. About two-thirds of the work was conducted from the road network below treeline, the remainder was by helicopter access, mainly near or above treeline. Approximately half of the geological mapping and sample collection was directed toward tenured lands in which Eagle Plains Resources Ltd. hold an interest. In the course of mapping, magnetic susceptibility of rock units and their altered or metamorphosed equivalents was routinely recorded in order to provide calibration for aeromagnetic data collected during past and future surveys. A total of 39 samples were collected for petrographic analysis (see photomicrographs that follow); 6 samples were collected for U-Pb geochronology (5 pending, data for one presented here), 9 samples were collected for $^{40}Ar/^{39}Ar$ geochronology (results pending); 54 samples were collected for assay by inductively coupled plasma – emission spectroscopy (ICP-ES) and instrumental neutron activation analysis (INAA), and 10 samples were collected for major and rare earth element analysis (REE results are pending).

Twenty-seven of fifty-four samples submitted for ICP-ES and INAA are reported, based upon their ICP-ES values, as follows: Au >500 ppb or Ag >1000 ppb or Cu, Zn, Pb >0.2%. Quality-control data are also reported. Note that the variation in Au and Ag ICP-ES values from the accepted standard was 101% and 8%, respectively, as a %RSD (relative standard deviation) measure. Variation in analytical results for duplicates averaged 89% and 36% (Au and Ag, Table 2). These uncertainties need to be considered during the following discussion on mineralization.

REGIONAL GEOLOGY AND PREVIOUS WORK

Duffell, Souther and others from the Geological Survey of Canada (GSC) conducted comprehensive geological work in the area in the late 1950s (Duffell and Souther, 1964). This remains the most complete written work published, although the GSC conducted several years of revision mapping, mainly in the mid-1980s (Woodsworth *et al.*, 1985), and topical thesis studies were completed. The most germane to exploration in the Kalum area is probably that of Heah (1991), which deals with contractional ductile and superimposed extensional deformation in the Shames River area, west of Terrace. A geological compilation by Evenchick *et al.*, (2004) and Massey et al. (2003) provide recent synoptic geological settings for the Kalum area. Geology west of Kalum Lake is detailed by Downie and Stephens (2003) on the Bootleg Exploration property. This latter report also provides an excellent overview of mineral exploration activity in the area west of Kitsumkalum Lake. For mineral occurrences east of the lake, the British Columbia Ministry of Energy and Mines MINFILE is the best source of information.

According to Woodsworth *et al.* (1985), the geology of the Kalum area is dominated by Middle to Late Jurassic marine deltaic and turbiditic strata of the Bowser Lake Group, as well as Lower Cretaceous fluvial-deltaic strata of the Skeena Group. A small window of Early Jurassic volcanic strata is preserved near the north end of Kitsumkalum Lake. All of these strata have been structurally thickened by gently south and north-dipping thrusts prior to extensive intrusion by mainly Cretaceous to Early Eocene magmatic bodies. Largest of these bodies is the huge, composite Ponder pluton (>1500 km^2 in British Columbia; Harrison *et al.*, 1978; Sisson, 1985; Van der Heyden, 1989), which lies outside the map area to the west. Numerous small intrusive bodies (<10 km^2) cut the deformed strata within, and east of, the Kitsumkalum valley.

Timing of thin-skinned fold and thrust deformation is best constrained by the Skeena Group and older rocks of the Skeena fold belt northeast of Terrace. Contractional deformation there is as old as Late Jurassic (Albian to Oxfordian), with final shortening of Latest Cretaceous or Paleocene age (Evenchick, 1991).

Structurally and magmatically thickened and thermally weakened parts of the Coast Belt continental arc were subject to extensional collapse in the Early Tertiary. In the southern Coast Belt, this occurred principally in Paleocene time (Friedman and Armstrong, 1988), whereas the event is dated as Paleocene to Eocene in the central Coast Belt near Terrace, (Andronicos *et al.*, 2003). Extensional collapse facilitated synorogenic emplacement of 60–50 Ma magmatic rocks, which constitute 25% of the crust over thousands of square kilometres in areas west and northwest of Terrace (Andronicos *et al.*, 2003).

STRATIGRAPHY

Four stratigraphic packages underlie the Kalum area: volcanic rocks correlated with the Early Jurassic Hazelton Group (Woodsworth *et al.*, 1985) and three clastic units belonging to the overlying Upper Jurassic Bowser Lake Group. Volcanic rocks include pillow basalt and structurally overlying calcareous tuff, which are exposed east of

northern Kitsumkalum Lake. These rocks have been affected by at least two phases of deformation (*see* 'Structure' section) and few protolith textures are preserved. No age data exist for these rocks within the Kalum area.

Bowser Lake Group strata in the Kalum area are dominated by one of three main lithologies: chert pebble conglomerate, sandy turbidites, or silty and carbonaceous argillite.

In roadcuts immediately west of the low mountain between northern Kitsumkalum Lake and the Mayo Creek valley (Fig. 2) are found the best exposures of chert pebble conglomerate (Fig. 3). Here, tabular to lensoid conglomerate units are interbedded with medium-grained arkosic sandstone and argillaceous siltstone. Elsewhere, chert pebbles are less abundant, occurring mainly within lags at the erosional bases of turbidite flow units. More commonly, the turbidite sequences are sand-dominated, lacking beds or lenses of chert pebble conglomerate. Turbidite successions are light grey to rusty-weathering. Typical turbidite sequences are composed of 2–6 m thick units with bases com-

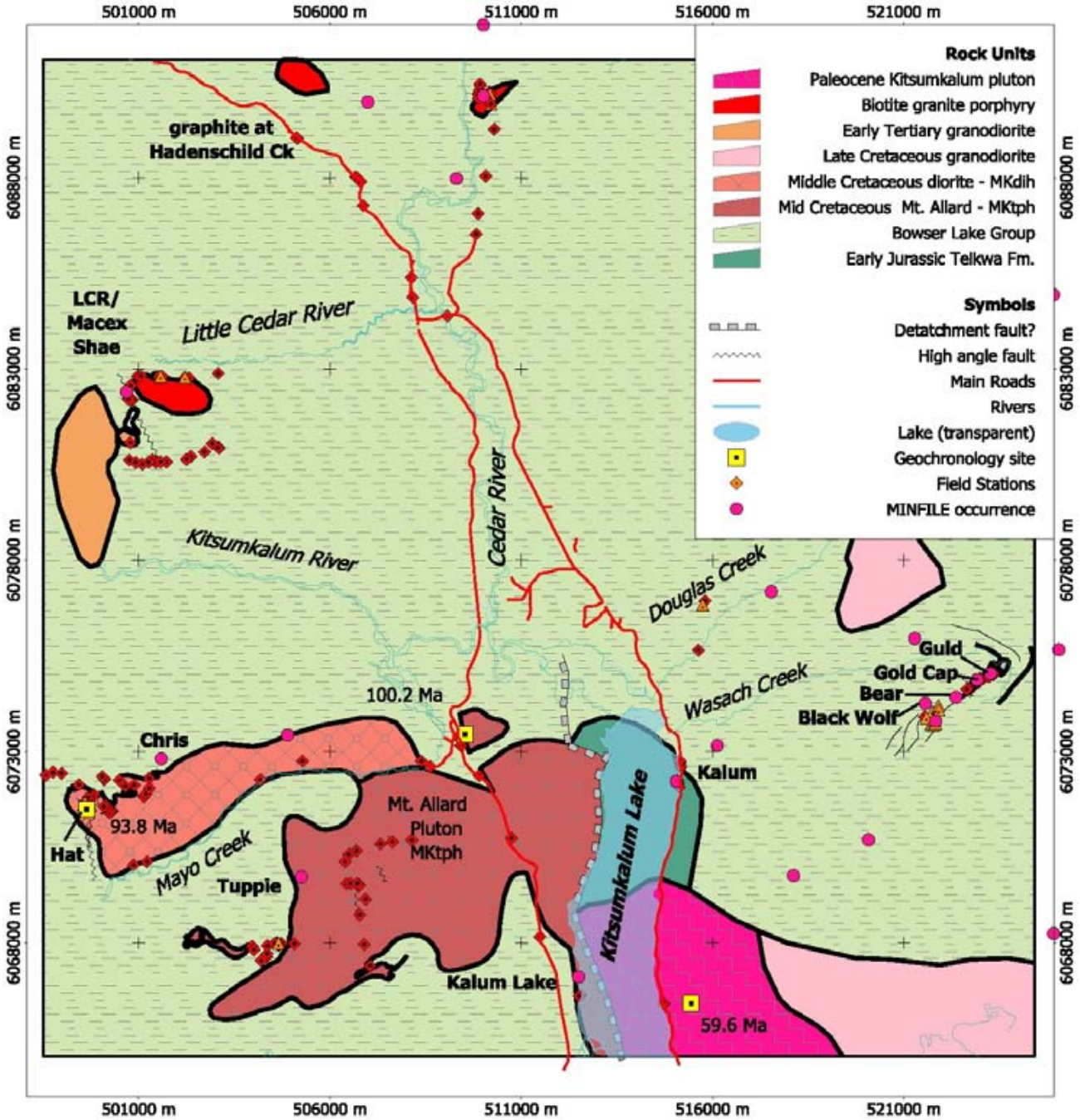

Figure 2. Generalized geology of the Kitsumkalum area. Sources of information: this project, Downie and Stevens (2003), Massey *et al.* (2003), and Woodsworth *et al.* (1985).

posed of rip-up clasts of underlying, dark brown argillite. Conglomerate grades up into medium to coarse-grained, planar-laminated light grey sandstone, parts of which may be interlaminated with millimetre-thick argillite. Laminated sandstone gives way up section to cross-stratified, clean lithic arkose. Cross-stratified sandstone constitutes at least 50% of each fining-upward unit, and they are overlain by silty argillite in which a high content of carbonaceous material is common. This argillaceous siltstone can attain thicknesses of several metres in both packages. It is commonly cut by slatey cleavage at a high angle to bedding. In a few localities, it can be mapped as a separate unit, tens of metres thick, that may include broad areas of pencil shale. Thermally metamorphosed, woody macerals can easily be mistaken for mica in hand samples. Such meta-macerals look like detrital mica that characterizes the Skeena Group. However, marine shelf and slope turbidites of the Bowser Lake Group can be distinguished on the basis of sedimentary facies from fluvial units that are more typical of the Skeena Group (C. Evenchick, personal communication, 2004).

INTRUSIVE PHASES

Semicircular plutons and tabular bodies, mainly of diorite to granodiorite composition, extensively intrude the Bowser Lake and older strata within the Kitsumkalum area. The volume of intrusions increases to the west, toward the Coast Plutonic Complex. Relative ages of the intrusive units are based upon crosscutting relationships, sparse geochronological data and degree of deformation. The latter criterion must be applied with caution because strong strain partitioning can impart fabrics to younger or synkinematic plutons while older, cold plutons are unaffected. The following intrusive phases are listed in presumed order of intrusion, from oldest to youngest.

Figure 3. Hornfelsed chert pebble conglomerate.

Poikilitic Hornblende Tonalite

Euhedral, poikilitic hornblende phenocrysts characterize this tonalite, which forms the Mount Allard pluton (Downie and Stephens, 2003; Fig. 4, unit MKtph). This pluton is a >35 km^2, homogeneous body. Poikilocrysts enclosed by hornblende are plagioclase (with strong oscillatory zoning) and opaque minerals (Fig. 4b). Lithologically similar dikes, locally hornblende megacrystic, may display strong foliation and/or carbonate alteration. The Mount Allard pluton cuts unit MKdih. A K/Ar (hornblende) cooling age of 100.2 ± 6.8 Ma reported for this body is (Godwin, unpublished in Breitsprecher and Mortensen, 2004). Alteration or possibly regional low-grade metamorphism of one

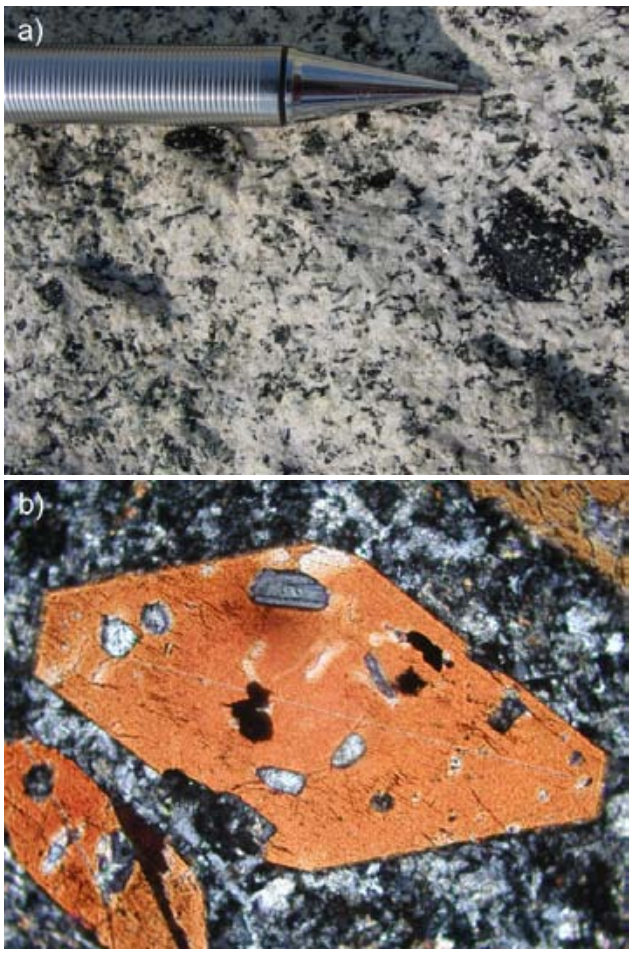

Figure 4. **a)** Typical texture of poikilitic hornblende porphyry of the Mount Allard pluton (unit MKtph). Note the weak magmatic fabric. **b)** Photomicrograph of euhedral hornblende with poikilocrysts of plagioclase and opaque minerals. Width of photo is ~4 mm.

fresh-looking outcrop is carbonate>prehnite~chlorite>epidote>?pumpellyite+ ?zoisite.

Hornblende-Pyroxene Quartz Diorite

A weak to strong foliation and local folding are displayed within this quartz diorite body (unit MKdih) in the northwestern part of the study area, just north of Mayo Creek. Quartz is interstitial to subidiomorphic and strained plagioclase that is weakly altered to carbonate, white mica and possibly prehnite. Pyroxene is the dominant mafic mineral; it is glomeroporphyritic and fresh. Hornblende is extensively altered to chlorite and pumpellyite. Folding is accommodated in part by slip along dense networks of discrete microfaults (Fig. 5). This body intrudes and thermally metamorphoses strata correlated with the Bowser Lake Group, a relative age that is confirmed by a U-Pb age of 93.8 Ma (*see* 'U-Pb Geochronology' section).

Quartz-Biotite Granite Porphyry

Quartz-biotite granite porphyry (unit Tpqb) may be the youngest intrusive phase in the Kalum area. It is exposed at low elevations in the Little Cedar River valley, near the LCR occurrence (Fig. 2). Relative age is based upon a lack of biotite hornfels, deformation fabric or regional metamorphic overprint. Locally, it is host to porphyry-style copper-molybdenum mineralization (Fig. 6) and has caused country rocks near its contacts to be locally replaced by sulphides (*see* below).

At higher elevations in the Little Cedar River valley, offshoots of the granite occur as rusty quartz-eye porphyry felsic dikes (unit Tpqhb) that contain 20% 1–3 mm tabular feldspar, 6% 5 mm acicular hornblende and 5% biotite. Quartz is up to 8 mm in diameter, coonstituting up to 5% of the rock. Pyrite is disseminated throughout and also occurs as sparse veinlets and blebs (up to 4% combined). These dikes apparently postdate folding inBowser strata because they parallel the axial surfaces of the folds.

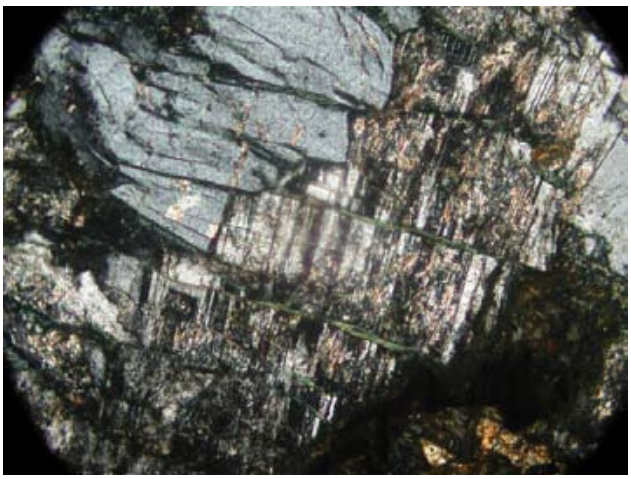

Figure 5. Microfaults in unit MKdih with apparent dextral offset cut a plagioclase-clinopyroxene grain boundary. Note intergranular quartz at the center-right edge of the photo. Width of photo is ~3 mm.

Kitsumkalum Pluton

Above the southeastern shores of Kitsumkalum Lake is a medium to coarse-grained, titaniferous metagranodiorite with enclaves of mafic schist, the Kitsumkalum pluton (Woodsworth *et al.*, 1985). It is of Paleocene age 59.6 +0.2/-0.1 Ma (Gareau *et al.*, 1997) and, notably, is much more strongly deformed than plutons dated more than 40 m.y. younger.

Dikes

Four phases of dikes repeatedly cut the sedimentary rocks and major plutons in the Kalum area. Based upon these crosscutting relationships, relative ages can be established.

Sugary aplite to graphic granite dikes with minor dikelet offshoots, which commonly have dark grey quartz-rich cores, occur in the Tuppie area, where they cut the Mount Allard pluton.

Acicular hornblende-feldspar porphyry dikes are common regionally. At least one variety cuts the Mount Allard pluton and dilatent quartz-carbonate veins (Fig. 7).

Chilled, very fine grained to aphanitic, dark green dikes look fresh and young, but may locally be affected by

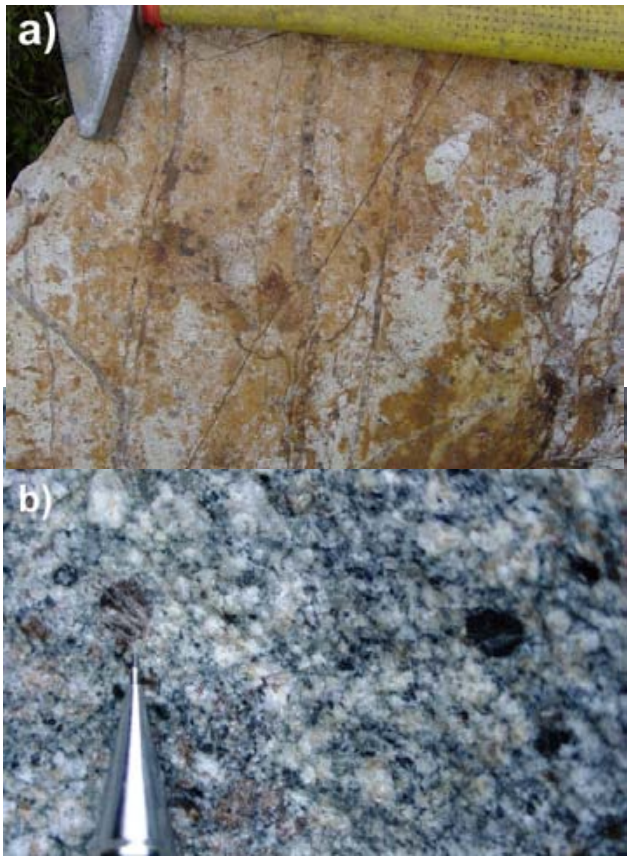

Figure 6. **a)** Sheeted quartz veins in bleached and rusty-weathering biotite-quartz porphyry (unit Tpqb) with disseminated chalcopyrite at the Shae occurrence. **b)** Representative view of unaltered porphyry showing a smokey quartz eye just above the pencil tip.

Figure 7. Acicular hornblende porphyry dike cuts dilatent veins and older mafic dike at the Tuppie occurrence.

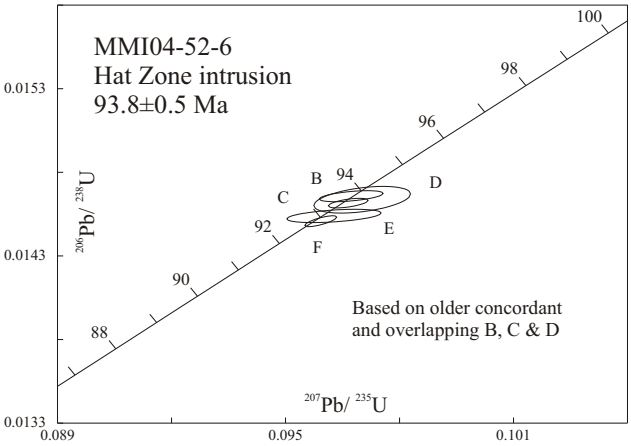

Figure 8. Concordia plot showing results for five zircon fractions from unit MKdih. The preferred interpreted age is 93.8 +/-0.5 Ma.

ductile deformation. Where they cut unit JKqdi, they form a swarm of 1–2 m thick bodies that consistently trend due north. Relative age with respect to other intrusive phases is not known.

Chilled, metre-thick lamprophyre dikes contain amygdules of a salmon pink mineral, tentatively identified petrographically as heulandite (low temperature zeolite). These dikes cut all structures within Bowser Lake strata and may be the youngest intrusive unit mapped in the area.

U-PB GEOCHRONOLOGY

Approximately 30 kg of unweathered pyroxene-hornblende quartz diorite was collected from near the Hat occurrence for determinion its crystallization age using the isotope dilution – thermal ionization mass spectrometry U-Pb method (ID-TIMS). All work was carried out at the Pacific Centre for Isotopic and Geochemical Research at the Department of Earth and Ocean Sciences, University of British Columbia. Mineral separation and U-Pb analytical techniques are given in Friedman *et al.* (2001). Results are plotted on a standard concordia diagram (Fig. 8) and listed in Table 1.

Results for five multigrain zircon fractions intersect the concordia between about 93 and 94 Ma. Slightly younger ages are attributed to very minor Pb loss, given the 1000–1800 ppm uranium concentrations of these zircons. A preferred age estimate of 93.8 ± 0.5 Ma is based on $^{206}Pb/^{238}U$ results for the three oldest concordant and overlapping fractions, B, C and D.

STRUCTURE

All layered rocks within the Kalum area have been affected by at least one phase of folding. Folds are open to close, although intrafolial isoclines are developed in the most ductile zones (Fig. 9). Faulting is common and obvious within both the Bowser Lake strata and the intrusive bodies.

Both concentric and similar fold styles are recognized within strata correlated with the Bowser Lake. Competent sandstone layers tend to act as beams and form concentric folds, except where they have folded at elevated temperatures. Argillaceous units tend to form similar folds, especially where graphitic. Intrafolial motion is ubiquitous within graphitic argillite, and these units are typically the locus of thrust fault flats.

Thrust faults developed within the Bowser Lake can be identified indirectly in incompletely exposed and isoclinally folded stratigraphy, where apparent fold limbs on either side of a hinge zone both face in the same direction. Thrust faults can be observed directly where they follow sheared bedding planes and then ramp upsection. Orientations of dilatent veins in the hangingwall of bedding-parallel faults can also be used to confirm thrust motion (Fig. 107). In rare instances, duplex structures with horses on the scale of metres to tens of metres long are well exposed. Slickensides on slip planes are less reliable indicators of thrust motion because they can also be formed by flexural slip, particularly in concentric folds, or during late minor fault motion related to unroofing or deglaciation.

Figure 9. Transposed layering and intrafolial isoclines near the eastern shore of northern Kitsumkalum Lake.

TABLE 1. ID-TIMS U-PB ANALYTICAL DATA FOR THE HAT ZONE PYROXENE-HORNBLENDE QUARTZ DIORITE

Fraction[1]	Wt	U[2]	Pb[*3]	$^{206}Pb/^{204}Pb$[4]	Pb[5]	^{208}Pb[6]	Isotopic ratios (1 ,%) [7]			Apparent ages (2 ,Ma) [7]		
	mg	ppm	ppm		pg		$^{206}Pb/^{238}U$	$^{207}Pb/^{235}U$	$^{207}Pb/^{206}Pb$	$^{206}Pb/^{238}U$	$^{207}Pb/^{235}U$	$^{207}Pb/^{206}Pb$
Hat Zone intrusion: age estimate of 93.8 ± 0.5 Ma based on $^{206}Pb/^{238}U$ dates for fractions B, C and D.												
B 6	0.014	1087	17	2216	6	17.7	0.01466 (0.11)	0.0967 (0.43)	0.04786 (0.39)	93.8 (0.2)	93.8 (0.8)	93 (18)
C 11	0.017	1232	20	5377	4	17.8	0.01462 (0.10)	0.0967 (0.27)	0.04796 (0.23)	93.5 (0.2)	93.7 (0.5)	97 (11)
D 8	0.012	1016	16	2281	5	17.0	0.01464 (0.27)	0.0970 (0.66)	0.04808 (0.59)	93.7 (0.5)	94.0 (1.2)	103 (28)
E 8	0.010	969	15	1004	9	18.0	0.01454 (0.14)	0.0963 (0.64)	0.04802 (0.60)	93.1 (0.3)	93.3 (1.2)	101 (28)
F 27	0.012	1784	28	5013	4	16.9	0.01451 (0.11)	0.0959 (0.22)	0.04796 (0.15)	92.9 (0.2)	93.0 (0.4)	97.1 (7.2)

[1] Upper case letter is zircon fraction identifier. All fractions were air abraded, with at least 20% volume removed. Selected zircons were greater than 100 micrometers, (dimension of longest axis), and were clear, pale pink, stubby prisms and tabular grains. Selected grains also contained internal c-axis parallel tubes extending much of their length. All grains were selected from the most non-magnetic split (nonmagnetic at 2 degrees sideslope and 2 amperes field strength on Franz™ magnetic separator; front slope 15 degrees). Progressively finer grains were selected for B-E; F comprises pieces of grains broken during abrasion. In the left column of the table each fraction is followed by the number of grains or grain fragmants dissolved.

[2] U blank correction of 1pg ± 20%; U fractionation corrections were measured for each run with a double ^{233}U-^{235}U spike (about 0.004/amu).

[3]Radiogenic Pb

[4]Measured ratio corrected for spike and Pb fractionation of 0.0037/amu ± 20% (Daly collector) which was determined by repeated analysis of NBS Pb 981 standard throughout the course of this study.

[5]Total common Pb in analysis based on blank isotopic composition.

[6]Radiogenic Pb

[7]Blank Pb was 1-3 pg throughout the course of this study; U <1 pg; common Pb composition for corrections based on Stacey Kramers (1975) model Pb at the age of the rock or the $^{207}Pb/^{206}Pb$ age of the rock.

LCR-Shae Area

Bowser Lake strata are intruded by quartz-phyric dikes, sills and stocks on the ridges above the LCR prospect. Good exposures extend for ~3 km eastward along the ridge from its contact with a body of hornblende-biotite granodiorite plus quartz diorite. Here, the Bowser strata are dominated by turbiditic units. Upright, open, north-northeast-trending concentric folds are intruded in their hinge zones by axis-parallel, rusty-weathering pyritic dikes that range in thickness from 1 to 5 m (intrusive unit Tpqhb). Farther west, folds apparently are of higher amplitude, with some fold axes occupied by thrust faults. At treeline to the east, an ~10 m thick sill (oriented 330 /30 is cut by a steeply dipping southeast-trending fault (133 /82 S) with southeast-side-down sense of motion (based on mapped offset in concert with slickensides on the fault surface). A strong lineament, which outlines the creek along which mineralization at the LCR is exposed, extends to a saddle in the ridge near UTM easting 501500 (Fig. 2) that is occupied by rusty-weathering argillaceous siltstone felsenmeer. No obvious change in lithology or in bedding orientation occurs across the saddle; however, it does mark the eastern limit of a zone of abundant dikes (rusty dikes of intrusive unit Tpqhb) with average orientations of ~200 /60 W. This orientation is parallel to fold hinges, suggesting a structural control.

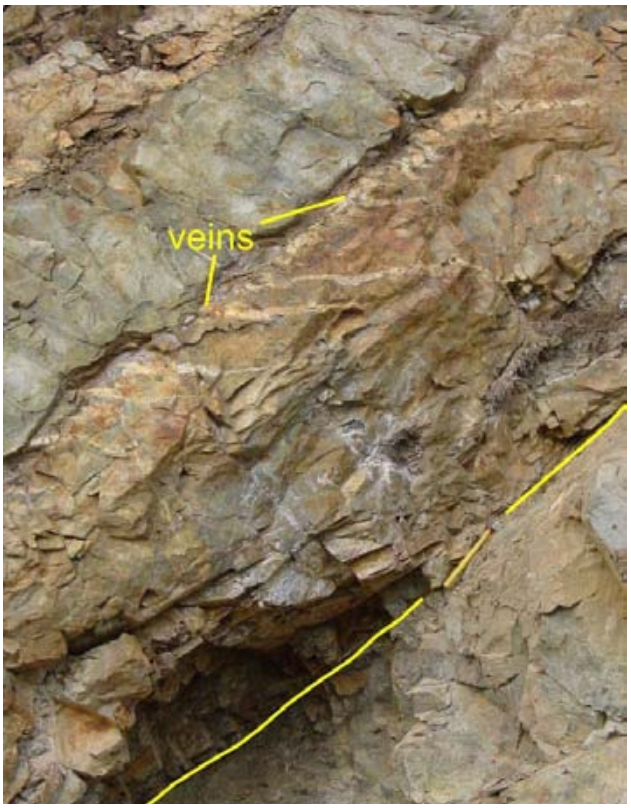

Figure 10. Dilatent quartz gash veins above thrust fault (at yellow hammer) indicate top-up-to-right (south) sense of motion, which is consistent with flat-ramp configuration (outside field of view).

Figure 11. Green, chlorite-altered brittle fault cuts orange carbonate alteration envelope around quartz veins.

Figure 13. North-dipping carbonate alteration zones on near horizon and on dark ridge beyond (north is to the right). Such zones host quartz-sulphide veins (arsenopyrite-pyrite-sphalerite-chalcopyrite-galena).

Mount Allard – Tuppie area

A weak magmatic foliation is common in the homogeneous Mount Allard pluton, but tectonic fabrics are also developed locally. For example, a scaly brittle fabric occurs in zones of chlorite alteration and magnetite destruction that are metres to tens of metres thick. These zones terminate at discreet brittle faults, measured in one locality at ~345 /75 . Brittle fault zones, with scaly chlorite, cut belts of extensive carbonate alteration within the pluton (Fig. 14). Carbonate alteration belts are range from several metres to ~12 m in thickness and are developed around sets of parallel quartz-carbonate veins that are generally less than 5 cm thick and oriented ~120 /80 S (Fig. 12).

Hat area

Deformation within the Hat area has resulted in open to close folds within turbiditic sandstone correlated with the Bowser strata. Tight intrafolial isoclines occur in rusty argillaceous strata and suggest that isoclinal folding has affected this fine-grained unit, at least at an outcrop scale. Folded strata are intruded by hornblende-pyroxene quartz diorite of unit MKdih, which has also been folded and is the dominant host to mineralization in the Hat area. Many mineralized veins dip at shallow angles and are clearly developed along brittle shears that dip shallowly to the north (~300 /30 N, 230 /20 N; Fig. 11, 13) and south (110 /30 S). At one locality, veins within the carbonate alteration zone appear folded and rodded (320 /20 N; Fig. 14). This type of folding may be restricted to hinge zones of folds that have straight limbs (*cf.* Fig. 13). If this is correct, the dominant limbs are north dipping, suggesting an overall south vergence.

Figure 12. Carbonate alteration of unit MKtph. Inset shows one of a minority of veins that are composed of euhedral quartz crystals growing into a cavity that was later infilled with calcite.

East of Kitsumkalum Lake

Rocks east of Kitsumkalum Lake are affected by ductile fabrics developed during at least two deformational events. These fabrics are well displayed by the border phases of the Kitsumkalum pluton. A pervasive strong foliation of ~200 /50 W (variable) contains a persistent mineral lineation ~250 /45 . Locally developed C^S fabrics indicate top-to-the-west sense of motion. Late brittle faults are oriented ~350 /60 E. All fabrics that affect the pluton must be younger than the age of the body, which is reported as 59.6 +0.2/-0.1 Ma (Gareau *et al.*, 1997).

East of the north end of Kitsumkalum Lake, retrograded calcareous chlorite schist (*see* next section) is deformed into south-verging, recumbent folds. Minor fold hinges defined by recessive carbonate layers, as well as ptygmatically folded quartz veins, display a dominant hinge orientation of ~070 /25 S. Subparallel with the long limbs of the enveloping folds are thrust faults (oriented ~240 /55 N) that were likely active during the folding event. Gash veins in the hanging walls of the thrusts are consistent with top-to-the-south motion on the thrust faults.

Figure 14. Carbonate alteration zone between the Hat and Chris prospects. This zone is more than 12 m thick and contains several arsenopyrite-pyrite-sphalerite-galena-chalcopyrite–bearing quartz-carbonate veins. Quartz rods in the foreground may have been produced by post-vein folding.

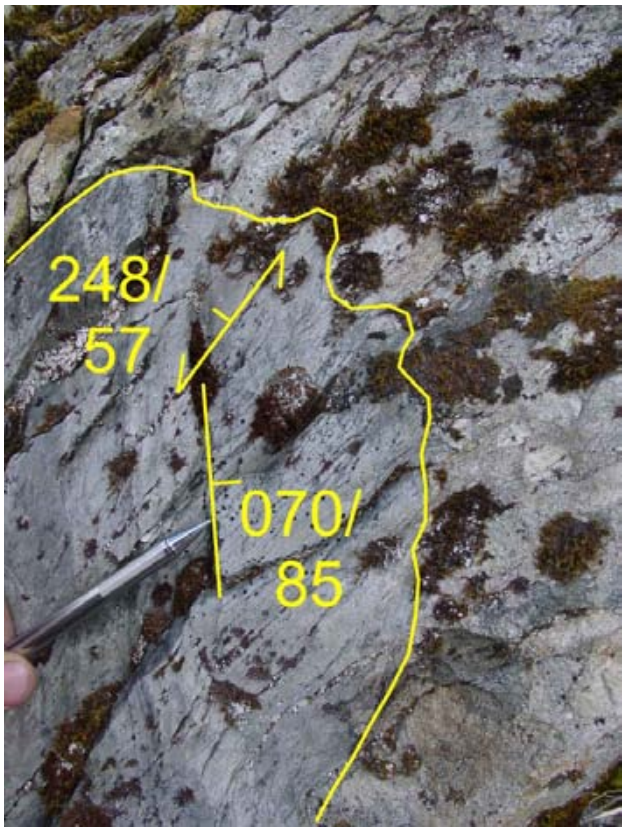

Figure 15. Well-bedded argillite in core of tight fold with straight limbs. Outside of fold is conglomerate. Clast elongation (050°/20°) is approximately parallel to resistant ridges underlain by conglomerate.

Folds with long limbs and tight hinges are typical of the sedimentary rocks hosting mineralization near the Black Wolf prospect, on the north flank of Maroon Mountain (*see* below). Mineralized veins appear to largely postdate this tight folding and follow the foliation that is at a low angle to bedding on the long limbs. Thus, veins appear in many places to be nearly concordant. These tight folds are, in turn, folded by an open kilometre-scale antiform with an east-northeast-trending axial trace (approximately parallel to Wasach Creek) that is interpreted based upon bedding orientations visible in airphotos and northwest-striking layers north of Wasach Creek.

METAMORPHISM

Biotite hornfels is the most common metamorphic facies within the Kalum area. Outside of the thermal metamorphic aureoles, a change in regional metamorphic grade occurs, with increases both west and east of the Kalum area. For example, sillimanite and granulite grades are attained to the west, within the Coast Belt (Sisson, 1985). East of northern Kitsumkalum Lake, retrograde spotted chlorite schist contains relicts of andalusite porphyroblasts with internal schistosity that is discordant with respect to the enclosing schistosity. In contrast, near Sand Lake to the north or along the Copper River to the southeast (Mihalynuk and Ghent, 1996), strata are metamorphosed only to zeolite facies.

MINERALIZATION

Mineral occurrences near Kitsumkalum Lake were examined during this study. Many are located on the Kalum and LCR properties held by Eagle Plains Resources and others on four crown grants on Maroon Mountain. We also report on newly discovered mineralization at the Shae occurrence, as well as newly discovered veins near the Hat prospect.

We investigated four styles of mineralization in the Kitsumkalum Lake area:

Type 1: porphyry-style copper-molybdenum-zinc vein stockworks in quartz-biotite granite porphyry at the Shea occurrence, and in adjacent country rocks

Type 2: semimassive sulphide replacement copper-zinc-molybdenum mineralization in clastic country rocks at the Shea occurrence

Type 3: quartz-polymetallic sulphide veins (zinc, lead, copper-silver-gold-arsenic), commonly within a carbonate envelope in an intrusive host at the the Hat and Tuppie occurrences

TABLE 2. INAA RESULTS FOR SELECTED ELEMENTS AND SELECTED SAMPLES

			Element	Au	Ag	As	Ba	Fe	Sb	Sc	W	Zn	La
			Units	ppb	ppm	ppm	ppm	%	ppm	ppm	ppm	ppm	ppm
Field			***Detect limit***	***2***	***5***	***0.5***	***50***	***0.02***	***0.1***	***0.1***	***1***	***50***	***0.1***
Number	**Sample Type**	**Easting**	**Northing**										
MMI04-44-20	LCR at PWLCV3	500784	6082170	27	-5	7.0	-50	2.72	1.5	0.6	-1	117	-0.5
MMI04-44-24	Shae sulphide blocks	501065	6082814	60	-5	5.8	240	13.7	1.7	8.9	-1	-50	15.2
MMI04-45-7	Kalum 65cm vein	512513	6066613	2305	214	427	-280	2.32	3270	0.5	-2	324	-0.5
MMI04-47-10	Tuppie qtz-py-cc (dike)	504653	6067933	8	9	27.4	780	3.61	12.5	9.5	6	183	-0.5
MMI04-47-10b	Tuppie qtz-sulphide vein	504653	6067933	880	44	11000	-310	1.41	2470	2.6	-2	9320	4.4
MMI04-47-8	Tuppie qtz-sulphide vein	504609	6068011	29	-5	296	-50	6.32	12.0	3.5	3	906	3.3
MMI04-48-10	Tojo -block from buttress	499833	6071878	1670	206	157	-50	1.79	676	2.2	7	5580	-0.5
MMI04-48-12b	Tojo -block from buttress	499680	6071795	1610	-24	42400	-650	8.51	-4.1	15.2	-4	-70	8.1
MMI04-48-13	Hat qtz-sulphide (aspy)	499559	6071473	1540	-30	93600	-970	10.3	-6.1	2.9	91	-87	-0.6
MMI04-48-14	Hat qtz-sulphide bx	499610	6071522	615	53	87.0	-50	4.96	61.3	2.8	-1	38200	-0.5
MMI04-48-14b	Hat qtz-sulphide bx block	499610	6071522	349	85	427	-50	2.14	141	1.5	-1	6130	0.9
MMI04-48-2	Hat E - carbonate altered	501186	6071889	6	-5	90.2	200	3.20	73.0	5.2	140	100	2.6
MMI04-48-3	Hat E - qtz-chl-? (black)	501275	6072040	453	-5	96.6	-50	1.52	3.7	0.8	3	63	1.4
MMI04-49-2	" 76cm chip, 62cm vein	500274	6071433	974	-12	26100	-380	9.19	208	3.8	1300	5300	8.9
MMI04-49-4	Hat E - qtz-gn vein	500186	6071472	47	8	71.4	170	1.45	13.3	1.2	7	265	2.1
MMI04-49-5	77cm chip, 42cm vein	500180	6071552	29	9	44.5	315	3.76	9.3	5.6	22	854	4.3
MMI04-49-8	4-22cm bx qtz-sulphide	499602	6071658	2220	56	765	581	3.96	27.3	10.4	16	32700	2.9
MMI04-49-8b	20 cm vein in block	499602	6071658	1450	194	15200	1100	4.50	284	3.4	294	51200	15.3
MMI04-49-9	Hat -sheared aspy-qtz	499620	6071620	1420	-14	23300	-245	6.68	24.6	20.8	49	11700	13.8
MMI04-50-5	grab - Kalum	515131	6072073	2940	-5	9.9	-35	6.08	2.0	27.0	-1	-50	4.2
MMI04-51-10	grab - Shae/LCR	501529	6082792	10	-5	5.5	301	1.00	0.3	1.5	-1	84	3.5
MMI04-51-5	grab - Big Joe	510211	6089930	166	-5	189	595	8.60	4.6	2.2	11	-50	16.5
MMI04-51-8	grab - Shae	502207	6082773	17	-5	6.1	126	8.36	0.3	15.4	6	130	13.1
MMI04-52-15	grab - Bear 10m trench/adit	522686	6074653	56200	129	78.8	-50	2.35	72.8	1.9	-1	297	1.8
MMI04-52-15R	grab - Bear 10m trench/adit	522686	6074653	55300	156	75.7	200	1.75	108	1.8	-1	286	1.7
MMI04-52-4	Hat -grab 1.3m bx vein	499669	6071516	462	104	345	-50	1.35	62.7	0.8	4	310	0.8
RFR04-3-13	grab - small adit	521922	6074080	57500	169	40.5	840	14.6	152	5.2	-1	27700	5.9
RFR04-3-9	grab - Black Wolf adit	521841	6073893	7600	104	225	-50	3.79	123	0.5	-1	5990	-0.5
QC													
	GSB Till 99 Std.			66	-5	55.4	590	6.0	14.1	23.6	-1	418	-0.5
	GSB Till 99 Std.			31	-5	50.1	990	6.2	10.9	23.6	-1	311	25.4
	GSB Till 99 Std.			38	-5	62.7	810	6.2	14.4	23.4	-1	319	-0.5
Mean				45	-5	56.1	797	6.1	13	24	-1	349	8
SD				19	0	6.3	200	0.1	2	0	0	60	15
% RSD				42	0	11.3	25	1.5	15	0	0	17	184
GSB Till 99	Recom. Values			**32**	**-5**	**61.7**	**827**	**8.2**	**13.4**	**29.9**	**-1**	**390**	**30.8**
58070	MMI04-52-15			56200	129	78.8	-50	2.4	72.8	1.9	-1	297	1.8
58076	MMI04-52-15R			55300	156	75.7	200	1.8	108	1.8	-1	286	1.7
% Difference				1.6	18.9	4.0	333.3	29.3	38.9	5.4	0.0	3.8	5.7
58133	MMI04-35-6			4	-5	13.1	950	3.9	1.7	9.9	-1	110	6.6
58136	MMI04-35-6R			15	-5	4.9	950	3.6	3.5	9.5	-1	116	6.0
% Difference				114	0	91.1	0	7.7	69.23	4.1	0	5.3	9.5

Table Notes: Coordinates are UTM Zone 9, NAD83
A full list of samples and elements analyzed can be obtained for both INAA (Table 2) and ICP-ES (Table 3) suites from: http://www.em.gov.bc.ca/Mining/Geolsurv/Publications/catalog/catfldwk.htm
QC = Quality Control

Type 4: lead-silver-gold veins, commonly in an argillite matrix; at the Guld, Gold Cap, Bear and Black Wolf occurrences

A variation of type 3 mineralization is seen at the Kalum Lake prospect, with elevated bismuth values, more typical of intrusive-related gold deposits.

Kalum Property

Three main styles of mineralization are seen on the Kalum property, west of Kitsumkalum Lake. One style of mineralization is a stockwork of quartz veins that contain sulphides, mainly chalcopyrite and pyrite, and appreciable molybdenite (type 1), south of the Little Cedar River (LCR). It is known as the Macex or LCR. A second style of

TABLE 3. ICP-ES RESULTS FOR SELECTED ELEMENTS AND SELECTED SAMPLES.

Field Number	Element / Detect limit / Sample Type / Units	Au 1 ppb	Ag 2 ppb	Cu 0.01 ppm	Pb 0.01 ppm	Zn 0.1 ppm	Mo 0.01 ppm	As 0.1 ppm	Mn 1 ppm	Fe 0.01 %	Cd 0.01 ppm	Sb 0.02 ppm	Bi 0.02 ppm	Ba 0.5 ppm	S 0.02 %	Hg 5 ppb	Se 0.1 ppm	Ga 0.02 ppm
MMI04-44-20	LCR at PWLCV3	44.2	2490	2722.51	2.61	91.9	>2000	-0.1	45	3.68	0.0	0.5	0.61	4.4	3.67	25	4.4	2.5
MMI04-44-24	Shae sulphide blocks	56.9	1303	2895.64	7.18	102.4	157.8	-0.1	441	15.09	1.0	0.1	2.89	31	8.33	-5	10.2	4.7
MMI04-45-7	Kalum 65cm vein	1221.3	>100000	4219.8	2879.61	284.5	1.44	226.7	35	2.29	3.9	>2000	559.87	34.6	1.16	6019	15.6	0.1
MMI04-47-10	Tuppie qtz-py-cc (dike)	2.3	6800	148.78	92.53	180.8	1.24	18.2	715	4.37	1.1	7.4	0.24	54.6	0.61	-5	0.3	3
MMI04-47-10b	Tuppie qtz-sulphide vein	636.5	27454	134.07	5344.66	9260.7	1.22	>10000	58	1.56	98.4	>2000	1.56	16.2	0.93	154	1.2	1.3
MMI04-47-8	Tuppie qtz-sulphide vein	27.9	1063	180.9	33.59	1221.1	17.5	417.7	979	8.27	13.2	5.9	2.03	11.4	1.48	11	3.1	6
MMI04-48-10	Tojo -block from buttress	1537.1	>100000	854.23	>10000	6706.7	1.65	127.7	78	2.06	59.7	724.5	0.09	18.5	1.55	425	0.7	0.4
MMI04-48-12b	Tojo -block from buttress	1238.2	690	5.3	9.66	68.4	0.53	>10000	1553	6.75	0.2	24.4	0.4	35.7	1.64	-5	1.6	7.1
MMI04-48-13	Hat qtz-sulphide (aspy)	1060.3	2342	48.42	39.04	59.1	3.47	>10000	634	9.92	1.2	80.6	0.97	28.4	4.98	17	4.4	1.2
MMI04-48-14	Hat qtz-sulphide bx	651.2	72090	205.11	5226.28	>10000	1.06	102.3	2525	7.26	475.4	72.3	0.04	10.3	4.76	735	0.7	2.7
MMI04-48-14b	Hat qtz-sulphide bx block	443.7	88429	173.61	1589.41	6770.9	0.57	465.8	517	2.37	64.3	127.1	0.02	10.9	1.37	161	0.1	0.8
MMI04-48-2	Hat E - carbonate altered	3.2	5400	93.97	15.71	98.9	0.36	88.8	1474	3.77	0.7	69.4	0.03	31.7	0.02	69	-0.1	0.9
MMI04-48-3	Hat E - qtz-chl-? (black)	1682.3	919	31.51	7.24	34.1	0.64	78.1	792	1.75	0.3	0.5	0.02	13.1	0.01	-5	0.1	2.2
MMI04-49-2	" 76cm chip, 62cm vein	1735.8	11400	83.45	1233.36	5600.8	2.11	>10000	5182	7.78	63.5	85.9	0.03	32	2.6	572	0.4	1.8
MMI04-49-4	Hat E - qtz-gn vein	26.1	8500	7.45	1241.58	198.3	0.76	70.4	548	1.55	1.1	7.1	-0.02	36.5	0.1	-5	0.1	0.4
MMI04-49-5	77cm chip, 42cm vein	25.5	12100	28.72	2974.55	931.7	3.36	42.9	1919	4.18	8.3	5.7	1.28	62.9	0.34	37	0.2	2.1
MMI04-49-8	4-22cm bx qtz-sulphide	3452.8	53000	358.4	1528.46	>10000	1.43	978	694	4.05	466.8	19.0	0.22	78.8	1.66	522	0.5	4.5
MMI04-49-8b	20 cm vein in block	1719.8	>100000	45.08	>10000	>10000	67.97	>10000	831	4.74	528.7	197.1	0.11	38.5	5.18	1585	2	1.5
MMI04-49-9	Hat -sheared aspy-qtz	1677.1	12100	145.81	1054.14	>10000	1.21	>10000	1528	6.41	211.7	31.6	0.33	81	2.45	229	1.1	3.3
MMI04-50-5	grab - Kalum	6152.2	8000	3152.18	5.98	60.2	0.59	8.2	561	3.79	0.4	0.7	4.93	98.2	0.03	7	1.4	3.8
MMI04-51-10	grab - Shae/LCR	3.4	662	740.25	1.79	58.8	6.92	1	163	1.19	0.6	0.1	0.18	30.4	0.34	-5	0.7	1.7
MMI04-51-5	grab - Big Joe	250.8	5600	267.65	50.05	24.4	1364	230.8	30	10.88	0.0	1.5	16.36	6.9	9.82	12	3.1	1.2
MMI04-51-8	grab - Shae	25.6	771	2252.41	6.39	142.4	30.8	-0.1	3007	9.09	0.3	0.3	4.55	16.4	4.08	-5	7	10.8
MMI04-52-15	grab - Bear 10m trench/adit	32456.3	>100000	170.74	>10000	331.2	1.04	61.4	30	2.28	1.5	60.9	11.54	11.6	0.61	81	9	0.2
MMI04-52-15R	grab - Bear 10m trench/adit	75827.7	>100000	198.12	>10000	340.7	1.06	78.1	27	2.47	2.0	100.4	17.69	13.3	1.02	149	14.9	0.3
MMI04-52-4	Hat -grab 1.3m bx vein	468.4	>100000	182.45	65.21	392.2	0.37	410	304	1.75	7.8	64.0	0.02	9.1	0.28	67	-0.1	1
RFR04-3_13	grab - small adit	>100000	>100000	3296.57	>10000	>10000	0.38	38.1	1836	19.07	356.5	154.2	0.39	28.9	>10	190	4.2	1.3
RFR04-3_9	grab - Black Wolf adit	11364.3	>100000	227.07	>10000	8096.5	0.41	312.1	360	5.31	85.3	148.3	0.44	5.5	6.25	121	3.8	0.7
QC																		
	GSB Till 99 Std.	15.9	1315	157.87	185.02	344.1	0.87	48.4	1408	6.29	0.7	7.9	0.23	262.6	-0.01	297	0.4	8.3
	GSB Till 99 Std.	124	1422	173.85	255.34	393	0.87	53.6	1583	7.48	0.7	9.2	0.25	292.3	-0.01	334	0.4	9.2
	GSB Till 99 Std.	20.6	1266	155.34	204	350.1	0.77	49.7	1306	6.49	0.6	7.8	0.22	266	-0.01	297	0.4	7.9
Mean		72.3	1344	164.595	229.67	371.55	0.82	51.65	1445	6.985	0.7	8.5	0.235	279.15	-0.01	315.5	0.4	8.55
SD		73.1	110.3	13.1	36.3	30.3	0.1	2.8	195.9	0.7	0.0	1.0	0.0	18.6	0.0	26.2	0.0	0.9
% RSD		101.1	8.2	8.0	15.8	8.2	8.6	5.3	13.6	10.0	6.4	11.2	9.0	6.7	0.0	8.3	0.0	10.8
GSB Till 99	Recom. Values	**28.60**	**1221.00**	**157.69**	**183.76**	**326.95**	**0.81**	**50.00**	**1288.0**	**6.30**	**0.64**	**7.59**	**0.22**	**233.60**	**-0.01**	**298.50**	**0.35**	**8.40**
58070	MMI04-52-15	32456.3	10000	170.74	10000	331.2	1.04	61.4	30	2.28	1.5	60.9	11.54	11.6	0.61	81	9	0.2
58076	MMI04-52-15R	75827.7	10000	198.12	10000	340.7	1.06	78.1	27	2.47	2.0	100.4	17.69	13.3	1.02	149	14.9	0.3
% Difference		80.1	0.0	14.8	0.0	2.8	1.9	23.9	10.5	8.0	29.4	49.0	42.1	13.7	50.3	59.1	49.4	40.0
58133	MMI04-35-6	12	203	39.72	24.4	59	0.68	12.1	708	1.95	0.2	1.1	0.35	342	-0.01	5	0.4	8
58136	MMI04-35-6R	4.1	434	46.21	98.12	62	0.51	4.9	650	1.9	0.2	2.6	0.63	284.8	0.02	9	0.4	7.5
% Difference		98.1	72.5	15.1	120.3	5.0	28.6	84.7	8.5	2.6	28.6	80.5	57.1	18.3	600.0	57.1	0.0	6.5

mineralization was discovered near the LCR property. Called the Shae occurrence, this mineralization is massive sulphide replacement of clastic strata (type 2; Fig. 16, 17). It is attributed to a mineralized quartz-biotite granite porphyry (Fig. 18) that might also be responsible for stockwork veining at the LCR. The most widely developed style of mineralization is base-metal sulphide-quartz (±carbonate) veins and networks of veins related to brecciation and shearing within zones of carbonate alteration (type 3; Fig. 19, 20).

Other zones of type 3 mineralization were discovered during mapping, mainly between the Hat and Chris occurrences, in areas recently exposed by the thaw of multiyear snow pack. There, additional arsenopyrite and base-metal sulphide veins within carbonate alteration zones were discovered (Fig. 17, 18).

HAT AREA

Tabular carbonate alteration zones are common between the Hat and Chris prospects. Chlorite-altered and folded hornblende-pyroxene quartz diorite is the main hostrock for mineralized veins in the Hat area. These zones range up to more than 12 m thick and typically contain multiple arsenopyrite-pyrite-sphalerite-galena-chalcopyrite–bearing quartz-carbonate veins (type 3). Mineralized quartz veins are commonly banded and brecciated, and form two sets, mainly oriented at low to moderate angles. Mineralization in low-angle veins occurs as massive coarse-grained sulphide (Fig. 19) or as mats of arsenopyrite needles that may be intergrown with sphalerite, galena and minor chalcopyrite (Fig. 20). One of the most impressive veins discovered during mapping was an ~20 cm thick vein consisting mainly of coarsely crystalline arsenopyrite, lesser sphalerite, galena and chalcopyrite, and broken quartz prisms, originally >10 cm long. Veins have been folded and sheared, and some sulphides appear to have been mobilized during these events, as indicated by the occurrence of chalcopyrite in microfactures oriented perpendicular to shear banding. Late gash veins oriented at a steep angle to the main sheared veins are generally not well mineralized.

LCR AREA – NEW SHAE OCCURRENCE

A logging road crosses an overgrown clearcut at an elevation intermediate between the main LCR mineralized zone and the Little Cedar River. Angular, rusty, sulphide-rich boulders containing up to 30% pyrrhotite and 2% chalcopyrite were found near the western termination of this road. Similar boulders were traced along the roadbed and colluvial banks for approximately 1.3 km to the east, down the valley to a mineralized outcrop (Fig. 14). This mineralization constitutes the Shae occurrence. The presence of mineralized boulders upstream and 'up-ice' of the known mineralized outcrops suggests that the boulders have not been transported by either river water or glacial activity. Consequently, a large mineralizing system is indicated.

Approximately midway between the end of the road and the easternmost mineralized outcrop (Fig. 16) is an exposure of biotite-quartz granite porphyry (unit Tqbp; Fig. 2, 18) with pyrite-chalcopyrite disseminated throughout and concentrated in a hydrothermal breccia zone roughly 20 cm thick. Massive sulphide replacement-style mineralization (Fig. 16) in outcrop and boulders is attributed to this mineralized porphyry body. A representative sample of the massive sulphide returned 2895 ppm Cu, 1303 ppb Ag, 157 ppm Mo (0.28% Cu, 1.3 g/t Ag, 0.015% Mo) and a trace of Au (57 ppb; Table 3, sample MMI04-44-24). The occurrence of mineralization over a distance of more than 1300 m indicates the Shae may be part of a large mineralizing system that warrants further investigation.

Isolated veins and vein stockworks at the LCR lack iron-stained carbonate alteration halos that accompany the base-precious metal veins elsewhere on the property. Instead, a grey clay-rich (?) halo appears to envelop some of the veins (these veins were not analyzed in detail, nor were they sampled for petrographic analysis). Veining at the LCR may be related to the mineralizing intrusion at the Shae occurrence.

Figure 16. Rich Friedman on a low roadcut outcrop of sulphide replacement-style mineralization at the new Shae occurrence.

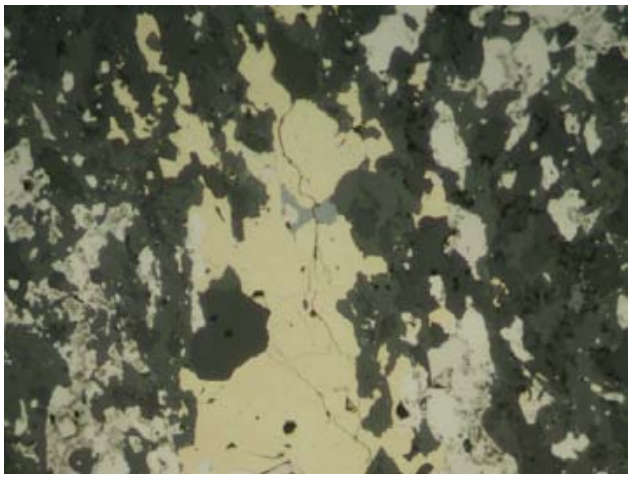

Figure 17. Reflected-light photomicrograph of replacement-style mineralization at the Shae occurrence. Yellow chalcopyrite with light grey inclusion of sphalerite; white mineral is pyrite; dark grey is gangue, mostly quartz. Field of view is ~0.9 mm.

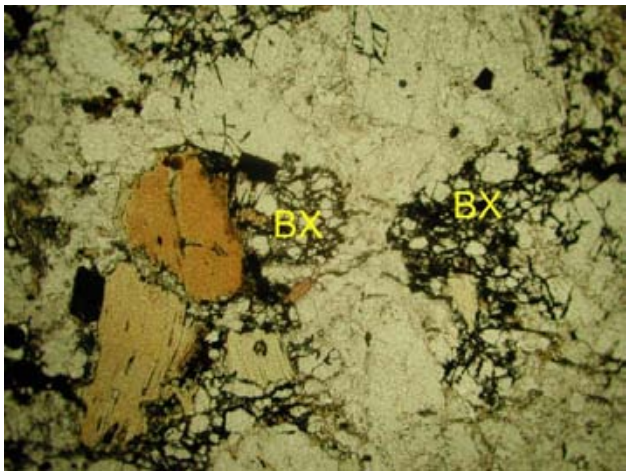

Figure 18. Photomicrograph of Fe-oxide > chalcopyrite cemented breccia zones (BX) within quartz-eye biotite porphyry at the Shae occurrence. Field of view is approximately 4 mm.


Figure 19. Jesse Campbell at a newly discovered ~15 cm thick arsenopyrite vein . This mineralization is exposed because of record-breaking thaws. Note relicts of the rapidly melting glacier in immediate background. A sample of the massive arsenopyrite vein is shown in the inset.

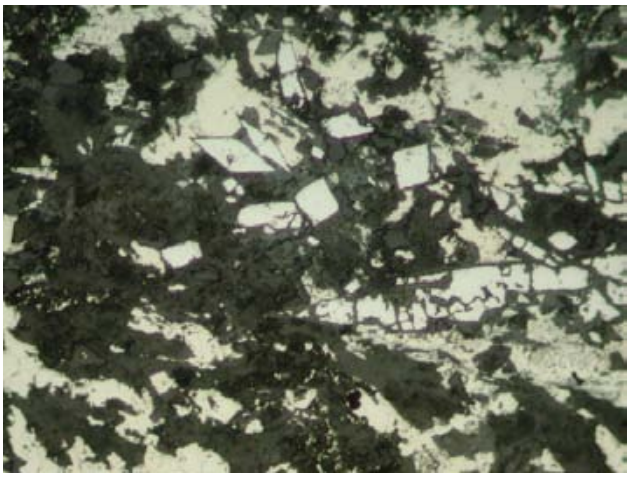
Figure 20. Highly reflective, slightly corroded, blue-white acicular needles of arsenopyrite, with diamond-shaped cross-sections, idiomorphic within white pyrite and yellowish chalcopyrite. Field of view ~0.9 mm.

TUPPIE AREA MINERALIZATION

The Tuppie showing is located at the western contact of the Mount Allard pluton, mainly in hornfelsed country rocks that are extensively crosscut by dikes. Petrographic observations show that pervasive chlorite alteration postdates carbonate alteration in some parts of the pluton. At the Tuppie showing, however, poikilitic hornblende megacrystic dikes are chlorite altered and then overprinted by carbonate alteration. Intensity of overprinting correlates with intensity of foliation fabric development, which increases near the sheared and strongly lineated eastern contact (150 /20). Silica and sulphides have accumulated at the eastern contact of one dike, probably late during the deformational episode because both are brecciated and annealed by quartz-carbonate and sulphide. A sample of foliated dike returned 6800 ppb Ag, in contrast to the immediately adjacent brecciated quartz vein that returned 27 454 ppb Ag and 636 ppb Au (Table 3, samples MMI04-47-10, 10b).

Zones of cryptic brecciation, up to 5 m across, occur within rusty, hornfelsed argillite. Black and rust, finely crystalline silica has flooded these zones. One grab sample of breccia returned values of 4400 ppb Ag (sample not listed in Table 2 or 3), indicating that such zones warrant further prospecting.

Maroon Mountain

Mineralization on the north flank of Maroon Mountain includes auriferous quartz and base-metal sulphide veins (type 4) that occur along a section a low ridge underlain near treeline by resistant conglomerate layers. Four occurrences listed in MINFILE are found along the northeast-trending ridge: Guld, Gold Cap, Bear and Black Wolf (from northeast to southwest, MINFILE #103I181, 028, 029, 030). Most MINFILE descriptions refer to the veins as concordant below a 35–75 m thick conglomerate layer. However, the conglomerate layer is tightly folded with hinges and clast elongation approximately parallel the northwest-trending (057º) ridge. The veins appear to largely postdate this folding and follow the foliation, which is at a low angle to bedding on the long limb.

Best assays were returned from two galena-rich quartz veins separated by an along-strike distance of 950 m (each about equidistant from the recorded location of the Bear occurrence; MINFILE 103I029). These are in the range 56 200 to >100 000 ppb Au (samples MMI04-52-15, RFR04-3-13; Tables 2 and 3). Orientation of the northern vein is 054 /58 S. It is a drusy, 35 cm thick, multistrand quartz-galena vein within graphitic phyllite. This vein is adjacent to a late, north-northwest-trending, high-angle fault with undetermined sense of motion.

Hadenschild Creek Graphite

Highway exposures of well-layered sedimentary strata immediately west of Hadenschild Creek are extensively cut by bedding-parallel faults. Typically, the faults are local-

ized in carbonaceous strata. Some display 30–50 cm of gouge, and within these fault zones are seams of graphite, commonly 20 cm thick. Impurities are locally scarce and are mainly calcite veinlets or fragmented veinlets. Graphite in the thickest seams is a homogeneous shiny grey and lacks anisotropy. Graphite quality test results are pending.

GEOCHEMICAL ANALYSES OF MINERAL OCCURRENCES

Keeping in mind the degree of analytical uncertainty for the ICP-ES and INAA analyses, some preliminary conclusions can be drawn. First, many of the mineral occurrences contain significant Au values. In fact, more than half of the 54 samples collected contain anomalous concentrations (greater than 40 ppb Au by ICP-ES). This includes mineral occurrences on both sides of Kitsumkalum Lake. For example, mineralized prospects on Maroon Mountain yield consistently high Au values. Surprisingly, these are higher than values reported in MINFILE. Similar lode veins in the area to the north are the likely source of placer gold in Douglas Creek, which has been recovered since the late 1800s.

INTRUSIVE-RELATED GOLD MODEL

Gold deposits that form during intrusion of magma into sedimentary strata rank amongst the largest known reservoirs of gold in the Earth's crust. These deposits fall into two major categories: 1) those hosted within or immediately adjacent to the intrusions (i.e., the intrusion-related/hosted or thermal aureole deposits); and 2) those hosted in sedimentary rocks, some of them many kilometres from the nearest known intrusion (i.e., the sediment hosted/Carlin type deposits; e.g., Lefebure and Ray, 1995). Contained gold values can be hundreds to thousands of tonnes. Famous sediment-hosted deposits, such as Muruntau in Uzbekistan (>5000 t; Morelli, 2004), Telfer in Australia (>450 t; Rowins *et al.*, 1997), and deposits of the Carlin trend in Nevada (Carlin, 320 t; Betze, ~1000 t; Meikle, >200 t;) tend to have grades in the range 3–14 g/t. Intrusion-hosted deposits, such as Kori Kollo in Bolivia (160 t; Long *et al.*, 1992), Fort Knox and Donlin Creek in Alaska (>200 t, Bakke, 1995; 775 t, Goldfarb *et al.*, 2004), or Dublin Gulch in Yukon (46.5 t, Yukon EMR, 2004) typically have gold grades around 0.5–3 g/t.

The role of magmatic fluids in sourcing and carrying gold is disputed, although most workers agree that intrusions provide the thermal gradient required to drive these mineralizing systems. Exploration for such deposits is guided regionally by their association with placer deposits and high-grade lodes (e.g., Dublin Gulch). Geochemical associations are elevated Au, Bi, Te, W ± (Mo, As, Pb) within or adjacent to the intrusion, and Au-As-Sb-Hg±(Ag, Pb, Zn) in distal deposits (Hart *et al.*, 2000, 2002). Currently accepted, broad application of the intrusive-related gold model includes distal, base, and precious metal veins (Au, Pb, Zn, As, Sb, Hg; Lang and Baker, 2001), which may point to a prospective intrusive system, if lacking merit as the base metal veins commonly do, in terns of grade and tonnage. Mineralizing fluids are reduced, with ore mineral assemblages containing arsenopyrite, pyrite or pyrrhotite, and lacking Fe-oxides. However, sulphide contents tend to be low overall (<5%; Lang and Baker, 2001). Carbon-dioxide–rich fluid exsolution during magma crystallization may be critical in destabilizing other ligands (e.g., bisulphide) that are responsible for Au solubility (Lowenstern, 2001). Evidence of carbonic fluid interaction is theoretically predicted and empirically verified in known deposits (Baker and Lang, 2001). Gold-rich intrusive systems have potential for huge gold resources. Consequently, they are attractive exploration targets. Features of mineralization in the Kalum area, particularly type 3 sulphide veins with carbonate alteration envelopes, are similar to those found within producing intrusion-related deposits.

DISCUSSION

By far the most common type of mineralization in the Kitsumkalum Lake area is polymetallic sulphide veins (type 3). These occur within and adjacent to both the Mount Allard pluton and diorite at the Hat occurrence. The intensity of carbonate alteration (±sulphide mineralization) may be enhanced by strain localization within the alteration zone. Quartz-carbonate veining in the Mount Allard pluton is not folded, but folding has definitely affected at least some of the veins in the Hat diorite. Fold styles may be similar to those seen on northern Kitsumkalum Lake and Maroon Mountain: long, fairly straight limbs and tight, relatively convolute hinges. However, our structural investigation was not extensive enough to permit unequivocal determination of the source of veins in the Hat intrusion. A possible linkage between mineralization and extensional structures needs to be further evaluated.

We originally considered the Hat diorite to be older than the Mount Allard pluton because it is more strongly deformed. However, available isotopic age data, if correct, indicate an inverse relationship between the degree of deformation and age of the intrusive body. Three age determinations are available for intrusive rocks in the Kalum area: a cooling age of 100.2 ± 6.8 Ma for the relatively undeformed Mount Allard pluton (Godwin, in Breitsprecher and Mortensen, 2004); 93.8 ± 0.5 Ma for the Hat diorite (reported here); and 59.6 +0.2/-0.1 Ma (Gareau *et al.*, 1997) for the strongly deformed North Kitsumkalum pluton. These relationships show that deformation did outlast Early Eocene plutonism. They also indicate that the degree of deformation in these bodies may be determined more by how much the pluton has cooled prior to deformation, or proximity to a ductile fault zone, than by how much/many of the deformational episode(s) the intrusion has experienced.

Polymetallic quartz-carbonate veins and alteration zones cut thermal metamorphic halos and plutons at least as young as the Mount Allard pluton. Mineralization cannot be attributed to the phases of the Mount Allard pluton that are cut by mineralized veins. However, exsolved fluids related to late crystallization of an interior phase of the pluton could explain veins within the roof of the pluton (cf. Clear

Creek in the Yukon; Marsh *et al.*, 2003). It is more difficult to attribute veins near the Hat prospect to the same intrusive source because the plutonic hostrocks there are clearly of a different composition.

Is epithermal veining related to (extensional) deformation a reasonable alternate to intrusion-related gold veins? Rapid changes in metamorphic grade and structural level, especially well displayed in the Kitsumkalum valley, are hallmarks of an extended terrain. Juxtaposition of low-grade rocks atop hotter, deeper level rocks through structural omission during extensional faulting could explain the lack of an intrusive body to which broad thermal metamorphism can be attributed. However, extension-related epithermal quartz-carbonate veins, such as those of the Republic Graben, typically contain only traces of sphalerite, galena and chalcopyrite. In contrast, veins in the Kalum area display mineralogy that is more typical of an intrusion association: base metal rich with elevated bismuth (cf. the Kalum Lake prospect). Even less equivocal is the porphyry association of veins at both the Shae occurrence and LCR/Macex, which display molybdenite mineralization in addition to chalcopyrite. At the Shae, the mineralizing biotite-quartz porphyry can be observed directly.

SUMMARY

Byproducts of geological mapping have been a preliminary evaluation of the regional structural deformational history. This history is far more complex than is indicated by existing published maps, although it appears to be similar to that recorded in the area immediately to the west by Andronicos *et al.* (2003) and in the unpublished M.Sc. thesis of Heah (1991).

Prospecting during the course of mapping resulted in notable new finds north of the LCR occurrence and near the Hat prospect. These are, respectively, porphyry and sulphide-replacement mineralization in angular boulders and outcrops along a >1 km transect, named the Shae occurrence, and several arsenopyrite and base-metal sulphide veins exposed in areas normally covered by snow and ice.

There are four styles of mineralization in the Kitsumkalum Lake area:

Type 1: porphyry-style copper-molybdenum-zinc vein stockworks in quartz-biotite granite porphyry and in adjacent country rocks

Type 2: semimassive sulphide replacement copper-molybdenum mineralization in clastic country rocks

Type 3: quartz-polymetallic sulphide veins (zinc, lead, copper-silver-gold), commonly within a carbonate envelope in an intrusive host

Type 4: lead-silver-gold veins, commonly in an argillite matrix

The abundance of type 3 veins east of the Hat occurrence and the richness of type 4 veins in the Maroon Mountain area underscore the presence of attractive intrusion-related mineralization that spans the range from proximal (type 3) to epizonal (type 4; e.g., Hart *et al*, 2002) veins.

ACKNOWLEDGMENTS

This field project would not have been possible without the generous financial contribution from our corporate partner, Eagle Plains Resources. Eagle Plains executives, Tim Termuende and Charles Downie, conceived the project. Project geologist Chris Gallagher, despite the demands of a new drill project, made time for geological discussions. Glen Hendrickson, Brad Robison and Jesse Campbell shared their personal knowledge of the Kalum area, as well as their home base in Terrace. Jesse Campbell also proved an able field assistant and prospector.

Dave Lefebure is thanked for his excellent editing skills in reviewing the manuscript.

Geochronological work is conducted in partnership with the Pacific Centre for Isotopic and Geochemical Research at the Department of Earth and Ocean Sciences, University of British Columbia, which is funded in part by NSERC grants.

REFERENCES

Andronicos, C.L., Chardon, D.H., Hollister, L.S., Gehrels, G.E. and Woodsworth, G.J. (2003): Strain partitioning in an obliquely convergent orogen, plutonism, and synorogenic collapse: Coast Mountains Batholith, British Columbia, Canada; *Tectonics*, Volume 22, pages 7-1–7-24.

Baker, T. and Lang, J.R. (2001): Fluid inclusion characteristics of intrusion-related gold mineralization, Tombstone-Tungsten magmatic belt, Yukon Territory, Canada; *Mineralium Deposita*, Volume 36.

British Columbia Ministry of Energy and Mines (2001): British Columbia Regional Geochemical Survey digital data, Terrace, 103I; *BC Ministry of Energy and Mines*.

Breitsprecher, K. and Mortensen, J.K. (2004): BCAge 2004A – a database of isotopic age determinations for rock units from British Columbia (Release 2.0); *BC Ministry of Energy and Mines*, Open File 2004-3.

Downie, C.C. and Stephens, J. (2003): Kalum gold-silver property; *BC Ministry of Energy and Mines*, Assessment Report 27 417, 54 pages (plus appendices).

Duffell, S. and Souther, J.G. (1964): Geology of Terrace map-area, British Columbia; *Geological Survey of Canada*, Memoir 329, 117 pages.

Evenchick, C.A. (1991): Geometry, evolution, and tectonic framework of the Skeena fold belt, north-central British Columbia; *Tectonics*, Volume 10, pages 527–546.

Evenchick, C.A., Mustard, P.S., Woodsworth, G.J. and Ferri, F. (2004): Compilation of geology of Bowser and Sustut basins draped on shaded relief map, north-central British Columbia; *Geological Survey of Canada*, Open File 4638.

Friedman, R.M. and Armstrong, R.L. (1988): Tatla Lake metamorphic complex: an Eocene metamorphic core complex on the southwestern edge of the Intermontane Belt of British Columbia; *Tectonics*, Volume 7, pages 1141–1166.

Friedman, R.M., Diakow, L.J., Lane R.A. and Mortensen, J.K. (2001): New U-Pb age constraints on latest Cretaceous magmatism and associated mineralization in the Fawnie Range, Nechako Plateau, central British Columbia; *Canadian Journal of Earth Sciences*, Volume 38, pages 619–637.

Gareau, S.A., Woodsworth, G.J., Friedman, R.M. and Childe, F. (1997): U-Pb dates from the northeastern quadrant of Terrace map area, west-central British Columbia; *in* Current Research, *Geological Survey of Canada*, Paper 1997-1A, pages 31–40.

Harrison, T.M., Armstrong, R.L., Naeser, C.W. and Harakal, J.E. (1978): Geology and thermal history of the Coast Plutonic Complex, near Prince Rupert, British Columbia; *Canadian Journal of Earth Sciences*, Volume 16, pages 400–410.

Hart, C.J.R., Baker, T. and Burke, M. (2000): New exploration concepts for country-rock-hosted, intrusion-related gold systems: Tintina Gold belt in Yukon; *in* The Tintina Gold Belt: Concepts, Exploration and Discoveries, Tucker, T.L. and Smith, M.T., Editors, *British Columbia and Yukon Chamber of Mines*, Special Volume 2, pages 145–172.

Hart, C.J.R., McCoy, D.T., Goldfarb, R.J., Smith, M.T., Roberts, P., Hulstein, R., Bakke, A.A. and Bundtzen, T.K. (2002): Geology, exploration and discovery in the Tintina Gold Province, Alaska and Yukon; *Society of Economic Geologists*, Special Publication 9, Chapter 6, pages 241–274.

Heah, T.S.T. (1991): Mesozoic ductile shear and Paleogene extension along the eastern margin of the Central Gneiss Complex, Coast Belt, Shames River area, near Terrace, British Columbia; unpublished M.Sc. thesis, *University of British Columbia*, 155 pages.

Lang, J.R. and Baker, T. (2001): Intrusion-related gold systems: the present level of understanding; *Mineralium Deposita*, Volume 36, pages 477–489.

Lefebure, D.V. and Ray, G.E. (1995): British Columbia mineral deposit profiles, Volume 2 - metallics and coal; *BC Ministry of Energy and Mines*, Open File 1995-20, 135 pages.

Lowenstern, J.B. (2001): Carbon dioxide in magmas and implications for hydrothermal systems; *Mineralium Deposita*, Volume 36.

Marsh, E.E., Goldfarb, R.J., Hart, C.J.R. and Johnson, C.A. (2003): Geology and geochemistry of the Clear Creek intrusion-related gold occurrences, Tintina Gold Province, Yukon, Canada; *Canadian Journal of Earth Sciences*, Volume 40, pages 681–699.

Massey, N.W.D., MacIntyre, D.G. and Desjardins, P.J. (2003): Digital map of British Columbia: Tile NM09 South-coast B.C.; *BC Ministry of Energy and Mines*, GeoFile 2003-4.

Mihalynuk, M.G., and Ghent, E.D. (1996): Regional depth-controlled hydrothermal metamorphism in the Zymoetz River area, British Columbia; *Canadian Journal of Earth Sciences*, Volume 33, pages 1169–1184.

Morelli, R.M. (2004): The age of gold mineralization at the Muruntau Au deposit, Uzbekistan, from Re-Os arsenopyrite geochronology; *Geological Society of America*, Annual Meeting, Program with Abstracts, page 444.

Rowins, S.M., Groves, D.I., McNaughton, N.J., Palmer, M.R. and Eldridge, C.S. (1997): A re-interpretation of the role of granitoids in the genesis of Neoproterozoic Au mineralization in the Telfer Dome, Western Australia; *Economic Geology*, Volume 92, pages 133–160.

Sisson, V.B. (1985): Contact metamorphism associated with the Ponder pluton, Coast Plutonic Complex, British Columbia; unpublished Ph.D. thesis, *Princeton University*, 345 pages.

Stacey, J.S. and Kramers, J.D. (1975): Approximation of terrestrial lead isotope evolution by a two-stage model; *Earth and Planetary Science Letters*, Volume 26, pages 207–221.

Van der Heyden, P. (1989): Jurassic magmatism and deformation; implications for the evolution of the Coast Plutonic Complex (abstract); *Geological Society of America*, Cordilleran Section, 85th annual meeting and Rocky Mountain Section, 42nd annual meeting, Abstracts with Programs, Volume 21, page 153.

Woodsworth, G. J., Van der Heyden, P. and Hill, M. L. (1985): Terrace East Map area; *Geological Survey of Canada*, Open File 1136.

Yukon Energy, Mines and Resources (2004): Dublin Gulch Property, *Yukon Minerals Development Department*, Mineral Property Update, 94 pages.